JOURNAL OF GUIDANCE, CONTROL, AND DYNAMICS
Vol. 31, No. 3, May–June 2008

Deflection-Limiting Commands for Systems with Velocity Limits

Yoon-Gyung Sung*
Chosun University, Gwangju 501-759, Republic of Korea
and
William E. Singhose†
Georgia Institute of Technology, Atlanta, Georgia 30332

DOI: 10.2514/1.32864

A new method to generate deflection-limiting commands for systems with velocity limits is presented and evaluated. In addition to limiting transient deflection, the command profiles reduce residual vibration for rest-to-rest motion of oscillatory systems with one dominant mode. A beneficial advantage of the command profiles is that they are described by closed-form functions of the system frequency, deflection-limiting ratio, velocity limit, actuator force-to-mass ratio, and desired move distance. The performance of the commands is evaluated with respect to move duration, transient oscillation energy, maximum transient deflection, and robustness to modeling errors. The proposed approach is illustrated with a numerical simulation of a benchmark system and experimentally validated on a bridge crane.

I. Introduction

APPLICATIONS such as rest-to-rest slewing of space structures that are characterized by low damping and limited fuel consumption requirements must perform large angle slewing without residual oscillations of elastic modes. Furthermore, transient deflection of the structure must be limited to avoid damaging and stresses. A related application is the transport of crane payloads using velocity-limited motors. The payload should arrive at the target location with very little oscillation, but it should also not swing for away from the desired trajectory during the maneuver. Even if a control command is properly designed for system flexibility, the command may not be accurately realized due to actuator dynamics. As a result, large transient amplitude and residual vibration may occur. Therefore, many control schemes have been proposed to suppress unwanted vibration and deflection in flexible systems. The objective is to design a command in such a manner that the desired rigid-body motion is performed while the flexible modes are not excited to a significant degree.

Several methods have been presented to generate command profiles that are time optimal [1–6], limit transient deflection [7], and limit fuel consumption [8–10] under reliable numerical optimization algorithms. Even though these methods are powerful, they have the drawback that a separate numerical optimization must be performed to generate the command for every maneuver. This drawback produces a reliability issue and a time delay at the start of every maneuver or requires the command profiles to be precomputed and stored for retrieval. Furthermore, nonlinear optimization methods are susceptible to being caught in local minima, so the real-time implementation is slowed further by the need for some process that verifies the accuracy of the candidate solutions [11].

Input shaping has demonstrated the ability to suppress vibration of flexible spacecraft and cranes [12]. As shown in Fig. 1, input shaping works by convolving a baseline command with a sequence of impulses. The convolution product is then used to drive the system. Recently, some practical advancements based on input shaping have been made by considering robustness [13], limitation of transient deflection [14,15], and fuel efficiency [16,17]. Most related to this work is a closed-form method [15] developed to avoid numerical optimization-based approaches. However, the previous closed-form method concentrated only on transient deflection limiting and residual vibration reduction. In this paper, an advanced procedure is proposed to control transient deflection and to reduce the residual vibration of flexible systems when the system is subjected to a velocity limit. Furthermore, experimental results verify the usefulness of the new procedure.

The proposed method uses two different negative input-shaping techniques [15,17]. The first method is a modified unity magnitude zero vibration (MUMZV) shaper that limits transient deflection by using a smaller impulse magnitude at the end. The other is a scaled unity magnitude zero vibration (UMZV) shaper designed with the same magnitude as the last impulse of the MUMZV shaper to guarantee maximum transient deflection remains below a specified level. The velocity limit is satisfied by adjusting the time location of the second negative shaper. During the period between the two shapers, there is a coasting period that has zero residual vibration. Then, the entire command shaper is determined by the rigid-body dynamics to accomplish the desired rest-to-rest maneuver with the satisfaction of deflection and velocity limits of flexible systems. The features of the proposed command allow it to be applied to space, as well as industrial applications. In fact, many actuators have velocity limits that require careful command development for accurate and reliable maneuvers.

The next section presents a method that generates analytic deflection-velocity-limiting (DVL) commands that are parameterized by the deflection limit, move distance, velocity limit, and force-to-mass ratio. Then, a performance evaluation is presented with respect to move distance and velocity limit using a benchmark system. Lastly, the performance of the proposed method is validated by experiments on an industrial bridge crane.

II. Analytic Deflection-Velocity-Limiting Commands

The closed-form generation of the proposed deflection-limiting command for systems with velocity limits is based on input-shaping concepts [18], negative shapers [19], and a deflection-limiting method [15]. The general input-shaping technique is briefly reviewed for only one flexible mode and no damping. The nondimensional residual vibration that results from a sequence of impulses being applied to the system can be expressed by

$$RV(\omega) = \sqrt{\left[\sum_{i=1}^{n} A_i \cos(\omega t_i)\right]^2 + \left[\sum_{i=1}^{n} A_i \sin(\omega t_i)\right]^2} \qquad (1)$$

Received 16 June 2007; revision received 22 October 2007; accepted for publication 22 October 2007.

*Associate Professor, Department of Mechanical Engineering; sungyg@chosun.ac.kr.

†Associate Professor, Woodruff School of Mechanical Engineering; singhose@gatech.edu.

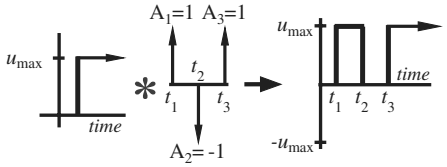

a) Unity magnitude zero vibration command

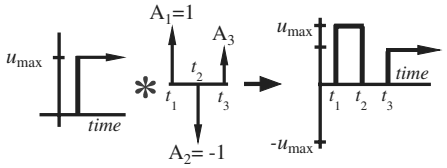

b) Modified unity magnitude zero vibration command

Fig. 1 Input shaping to generate zero vibration commands.

where ω, A_i, and t_i are a system's natural frequency, the amplitude and time location of the ith impulse, and n is the number of impulses in the impulse sequence. To make the residual vibration zero, the impulse amplitudes and time locations in Eq. (1) must satisfy

$$\sum_{i=1}^{n} A_i \cos(\omega t_i) = 0 \quad \text{and} \quad \sum_{i=1}^{n} A_i \sin(\omega t_i) = 0 \tag{2}$$

By setting the residual vibration to zero in Eq. (1) and solving for a positive two-impulse shaper, one obtains a ZV shaper [20]. To increase the robustness of input shaping to modeling errors, additional constraints are needed resulting in shapers with additional impulses [18].

Many shapers have been presented using the constraint of positive impulse amplitudes. However, a UMZV shaper [19] with one negative impulse amplitude can be defined when a unity magnitude constraint is combined with the zero vibration requirement. Thus, the UMZV shaper is expressed as a sequence of impulses given by

$$\begin{bmatrix} A_i \\ t_i \end{bmatrix} = \begin{bmatrix} 1 & -1 & 1 \\ 0 & \frac{T}{6} & \frac{T}{3} \end{bmatrix} \tag{3}$$

where T is the period of system vibration. As a special case of input shaping, the input shaper in Eq. (3) is convolved with a step input to form an on–off command that will lead to zero residual vibration, as shown in Fig. 1a. The duration of the UMZV shaper is shorter than the ZV shaper. However, if the shaped command needs to control excessive transient deflection, then the impulse magnitude requirement must be modified.

Figure 1b shows one form of the deflection-limiting shaper applied to a step command. The final value of the shaped step input is lower than the original value. Therefore, when the shaped step command is used in place of the original step command, the final deflection is smaller. By using Eq. (2) and setting the first impulse time, $t_1 = 0$, without loss of generality, the MUMZV shaper can be obtained as [15]

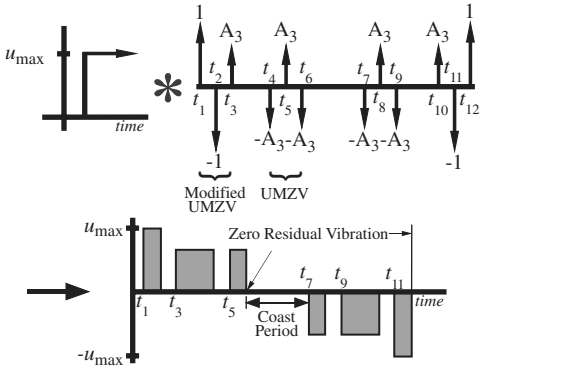

Fig. 2 Deflection-velocity-limiting command.

$$\begin{bmatrix} A_i \\ t_i \end{bmatrix} = \begin{bmatrix} 1 & -1 & A_3 \\ 0 & t_2 & t_3 \end{bmatrix} \tag{4}$$

where

$$t_2 = \frac{1}{\omega}\arccos(1 - 2D_L^2)$$

$$t_3 = \frac{1}{\omega}\arccos(-D_L)$$

and $D_L = A_3/2$ is the deflection ratio between the acceptable deflection and the maximum deflection resulting from a step input.

Equations (3) and (4) are used in this paper to generate the DVL commands for flexible systems. Given that a rest-to-rest maneuver is antisymmetric with regard to the midpoint of the maneuver time, the DVL shaper proposed here has 12 command switch times, as shown in Fig. 2, and is represented as an input shaper by

$$\begin{bmatrix} A_i \\ t_i \end{bmatrix} = \begin{bmatrix} 1 & -1 & A_3 & -A_3 & A_3 & -A_3 & -A_3 & A_3 & -A_3 & A_3 & -1 & 1 \\ t_1 & t_2 & t_3 & t_4 & t_5 & t_6 & t_7 & t_8 & t_9 & t_{10} & t_{11} & t_{12} \end{bmatrix}$$

The 12 command switch times are determined by enforcing the velocity limit of a system and using the rigid-body dynamics to move the system to a target location. The strategy devised here is to design the first half of the command to control deflection magnitude and to constrain system velocity by determining the switch times, t_4 and t_7. Hence, the gap between the UMZV and the MUMZV shapers is related to the velocity limit.

To compute the beginning time of the second half of the command (the deceleration), the midpoint time of a maneuver is expressed by

$$t_m = \frac{(t_6 + t_7)}{2} \tag{5}$$

where t_6 and t_7 are the times of the last positive pulse in the acceleration phase and the beginning negative pulse in the deceleration phase as shown in Fig. 2. If a system has mass M and the position of the system's center of mass is x, then the rigid-body equation of motion is expressed by

$$\ddot{x}(t) = u(t)/M \tag{6}$$

The first half of the DVL command $u(t)$ can be expressed as

$$u(t) = 1 - H(t - t_2) + A_3 \sum_{i=3}^{6} (-1)^{(i+1)} H(t - t_i) \tag{7}$$

where H denotes the Heaviside function. Starting from rest and solving the integral of Eq. (6) with Eq. (7) up to the midpoint time and setting it equal to the velocity limit (V_L), yields

$$V_L = (-t_3 + t_4 - t_5 + t_6)\alpha A_3 + \alpha t_2 \tag{8}$$

where α is the force-to-mass ratio. Performing another integration with respect to time, the position at midmaneuver can be set to one-half of the desired move distance, x_d:

$$\frac{x_d}{2} = \left\{(-t_3 + t_4 - t_5 + t_6)\alpha t_m + \frac{1}{2}(t_3^2 - t_4^2 + t_5^2 - t_6^2)\alpha\right\} A_3 - \frac{1}{2}\alpha t_2^2 + \alpha t_2 t_m \tag{9}$$

Using Eq. (3), t_5 and t_6 can be expressed as

$$t_5 = t_4 + T/6 \quad \text{and} \quad t_6 = t_4 + T/3 \tag{10}$$

Then, the switch time, t_4 can be determined from Eq. (8) using Eq. (14):

$$t_4 = t_3 - \frac{T}{6} + \frac{1}{A_3}\left(-t_2 + \frac{V_L}{\alpha}\right) \tag{11}$$

Substituting Eqs. (5), (10), and (11) into Eq. (13) and solving for t_7 gives

$$t_7 = \frac{N_1 \alpha A_3 + N_2 \alpha + 36 x_d}{6\alpha D} \tag{12}$$

where

$$N_1 = 12t_3(-3t_3 + 3t_4 + T) - 6t_4 T + T^2$$
$$N_2 = 12t_2(3t_2 - 3t_4 - T) \qquad D = 6t_2 + (-6t_3 + 6t_4 + T)A_3$$

By antisymmetry, the switch times for the deceleration command are obtained in closed form:

$$t_8 = t_7 + t_6 - t_5, \qquad t_9 = t_7 + t_6 - t_4, \qquad t_{10} = t_7 + t_6 - t_3$$
$$t_{11} = t_7 + t_6 - t_2, \qquad t_{12} = t_7 + t_6 \tag{13}$$

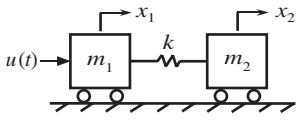

Fig. 3 Benchmark flexible system.

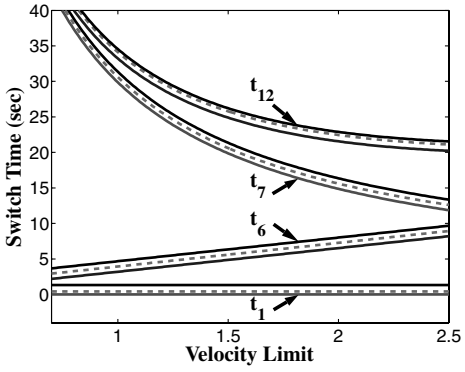

Fig. 4 Command switch times vs velocity limit.

The entire DVL command is described in closed form by Eqs. (4) and (10–13). The advantages of the closed-form commands will be addressed in the next section in terms of fuel savings, robustness to modeling errors, and decreased maximum transient deflection as a function of either move distance or velocity limit. Comparisons will be made to specified fuel and bang–coast–bang (BCB) commands.

Note that the closed-form commands calculated for very small move distances can cause overlapping of the impulse time sequences within the transition period so that the vibration cancellation does not occur perfectly. To eliminate this issue, the bound of the velocity limit should satisfy

$$V_L < \frac{(\alpha A_3 T)^2}{9} + (t_2^2 - 2t_2 t_3 A + t_2^2 A_3)\alpha^2 + \alpha A_3 x_d - \frac{\alpha A_3 T}{18}[3\alpha^2 A_3^2 T^2 + \{(-72t_2 t_3 + 36t_2^2)\alpha^2 + 36\alpha x_d\}A_3 + 36\alpha^2 t_2^2]^{1/2} \tag{14}$$

Furthermore, the bound of the move distance is

$$x_d > \left(\frac{-T^2 A_3}{18} + 2t_2 t_3 - t_2^2 - \frac{t_2^2}{A_3}\right)\alpha + \frac{V_L T}{3} + \frac{V_L^2}{\alpha A_3} \tag{15}$$

The bounding Eq. (15) prevents t_6 from being larger than t_7. With the benchmark flexible system in Fig. 3 where the command, $u(t)$, is designed as a rest-to-rest motion with limited vibration both during and at the end of the maneuver, the command switch times display a predictable dependence on the velocity limit. Figure 4 shows this dependence when $m_1 = 1$, $m_2 = 1$, $k = 1$, $x_d = 30$ units, $D_L = 0.3$, and $\alpha = 0.5$. As the velocity limit increases, the ending impulse time, t_6, of the acceleration region approaches the starting impulse time, t_7, of the deceleration.

III. Evaluation of Command Profiles

For the comparison of the proposed commands against references, specified fuel (SF) commands [17] and BCB commands are employed. The SF command can specify the amount of fuel usage for the desired move distance. The smaller the fuel usage, the longer the maneuver time. However, the SF command does not directly limit the transient deflection. To generate the same move distance, x_d, with the velocity limit, V_L, the complete SF shaper that is convolved with a step input can be expressed as

$$\begin{bmatrix} A_i \\ t_i \end{bmatrix} = \begin{bmatrix} 1 & -1 & 1 & -1 & -1 & 1 & -1 & 1 \\ 0 & \frac{U}{4} & t_3 & t_3 + \frac{U}{4} & t_5 & t_6 & t_7 & t_8 \end{bmatrix} \tag{16}$$

where U is the desired fuel usage in seconds,

$$t_3 = \frac{(2m+1)T}{2}, \qquad t_5 = \frac{2x_d}{\alpha U}, \qquad t_6 = t_5 + \frac{U}{4}, \qquad t_7 = t_5 + t_3$$
$$t_8 = t_5 + t_3 + \frac{U}{4}, \qquad U = \frac{2V_L}{\alpha}$$

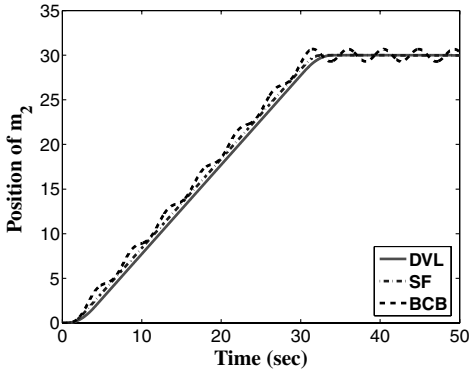

Fig. 5 Position responses of second mass.

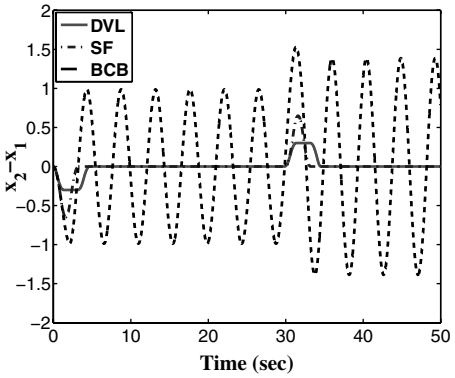

a) Deflection responses of m_2

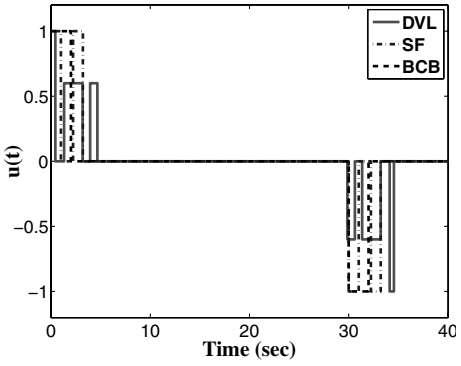

b) Input commands

Fig. 6 Deflection time responses of $x_2 - x_1$ and control inputs

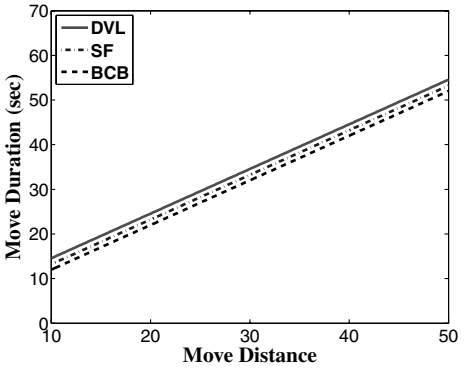

Fig. 7 Move duration vs move distance.

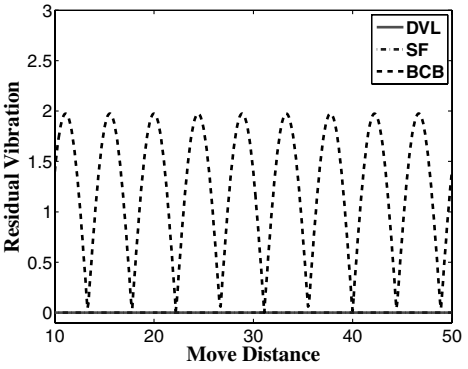

Fig. 8 Residual vibration vs move distance.

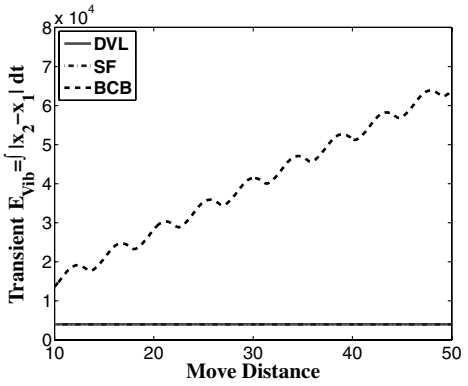

Fig. 9 Transition vibration energy vs move distance.

and $m = 0, 1, 2, \ldots$ is determined from the amount of given fuel so that the shaper sequences do not overlap. Note that observing a fuel usage limit with the above command is equivalent to observing a velocity limit.

The BCB command is assumed to begin at $t_1 = 0$ and is designed to produce the same final move distance, x_d, and velocity limit, V_L. The positive pulse for the acceleration from rest is ended at time t_2 and the negative pulse for the deceleration to rest is started at time t_3 which can be determined by the rigid-body dynamics. The entire BCB command is described by

$$\begin{bmatrix} A_i \\ t_i \end{bmatrix} = \begin{bmatrix} 1 & -1 & -1 & 1 \\ 0 & \frac{V_L}{\alpha} & \frac{x_d}{V_L} & \frac{V_L^2+\alpha x_d}{\alpha V_L} \end{bmatrix} \tag{17}$$

In Eqs. (16) and (17), x_d, α, and V_L are defined as before. The BCB command moves the center of mass to the desired position, however, significant residual vibration can be expected when the commands are applied to flexible systems. With the system parameters of $m_1 = 1$, $m_2 = 1$, $k = 1$, $x_d = 30$ units, $D_L = 0.3$, $V_L = 1.0$, and $\alpha = 0.5$, Fig. 5 shows the time response of the second mass. The BCB command produces oscillation during the transient period and residual vibration after the end of the move. On the other hand, Fig. 6a shows that both DVL and SF commands produce no visible oscillation during the coast period and no residual vibration after the desired move distance is achieved. However, the SF command produces larger transient deflection than the DVL command, as expected. Figure 6b shows the three input commands used to generate Fig. 6a. It shows that the move duration with the SF command is slightly shorter than with the DVL command.

Hereafter, the evaluation of the DVL commands, the SF commands, and the BCB commands uses the benchmark undamped flexible system shown in Fig. 3. The system parameters of $m_1 = 1$, $m_2 = 1$, $k = 1$, $D_L = 0.3$, and $\alpha = 0.5$ are fixed and the rest of the command parameters, such as move distance x_d and velocity limit V_L are varied to make performance comparisons.

A. Dependence on Move Distance

To evaluate the performance as a function of move distance, the velocity limit ($V_L = 1.0$) was fixed and then move duration, transient vibrational energy, residual vibration, maximum deflection, and insensitivity were evaluated by varying the move distance x_d.

As a performance measure of operational speed, Fig. 7 shows the move duration as a function of the move distance. As expected, the DVL command produces slightly longer move times than the SF and BCB commands throughout all of the move distances. As mentioned before, the SF and BCB commands were designed with the same velocity limit as the DVL command. The longer maneuver time of the DVL command as compared to the SF and BCB commands is compensated for by superior performances in the other performance measures.

Figure 8 shows that the BCB commands induce large residual vibration magnitude. With the given set of system parameters, the BCB commands periodically produce no residual vibration. However, the DVL and SF commands produce zero residual vibration for all move distances.

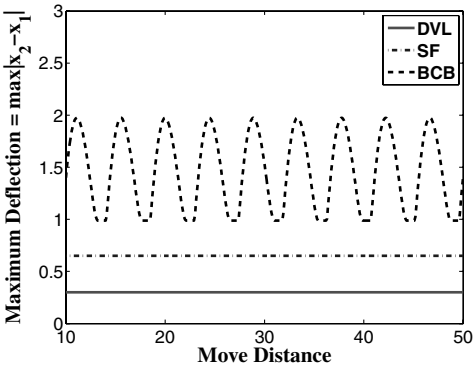

Fig. 10 Maximum deflection vs move distance.

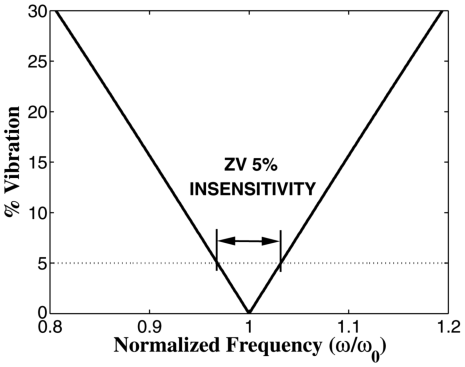

Fig. 11 Illustration of 5% insensitivity.

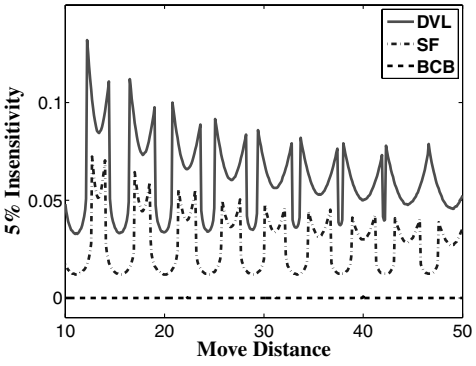

Fig. 12 The 5% insensitivity vs move distance.

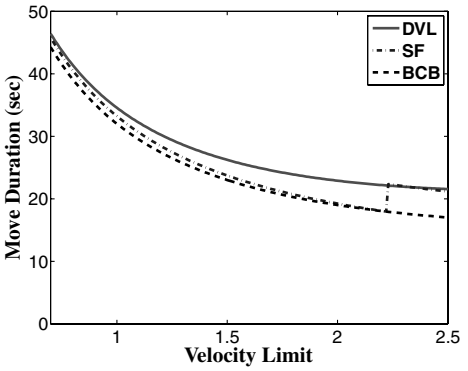

Fig. 13 Move duration vs velocity limit.

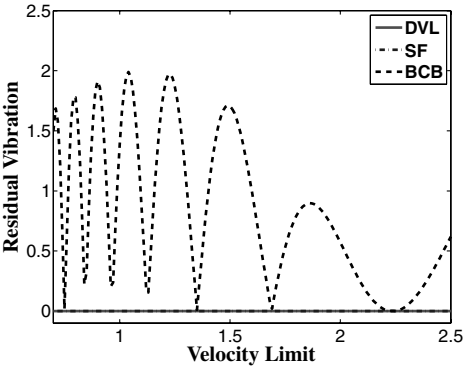

Fig. 14 Residual vibration vs velocity limit.

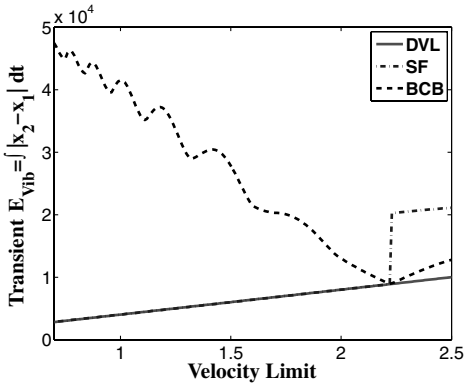

Fig. 15 Transition vibration energy vs velocity limit.

As an indirect measure of vibration, Fig. 9 shows the integral of the system deflection. The BCB command produces much more oscillation during the transient period than the DVL and SF commands. As the velocity limit is increased, the transient deflection increases for the SF command, as will be shown later.

A very important performance measure is the transient deflection, which can impact the lifetime of structures. In fact, large deflection may cause critical damage to structures or, in the case of a crane, cause the payload to swing into an obstacle. Figure 10 shows the maximum transient deflection as a function of move distance. The DVL commands induce 120% less deflection than the SF and average 400% less deflection than BCB commands. An interesting feature is that the deflection induced by the DVL and SF commands is constant for the entire range of the move distances. On the other hand, the BCB command induces large deflections that fluctuate with move distances. At certain distances, the BCB command induced 5.6 times more deflection than the DVL commands.

Because of modeling errors or uncertainty in the flexible mode, robustness is another important measure. A sensitivity curve showing the residual vibration amplitude resulting from modeling errors is shown in Fig. 11. The horizontal axis indicates the degree of modeling error by showing the actual frequency ω divided by the modeling frequency ω_0. The width of the curve that lies below at a tolerable vibration level is defined as the insensitivity to frequency errors. The 5% insensitivity indicates what frequency range will have vibration below 5% of the vibration induced by a step input. The 5% insensitivity as a function of the move distance is shown in Fig. 12. The DVL command has better robustness than the SF commands. The BCB commands have virtually zero robustness because the BCB commands are not designed to suppress residual vibration.

B. Dependence on Velocity Limit

For the evaluation of dependence on velocity limit, the move distance ($x_d = 30$ units) was fixed and then move duration, transient vibrational energy, residual vibration, maximum deflection, and insensitivity were evaluated as a function of the velocity limit.

Figure 13 shows move durations of all three commands as a function of the velocity limit. The system speed increases with

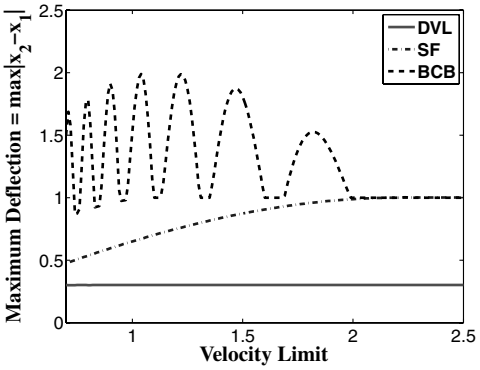

Fig. 16 Maximum deflection vs velocity limit.

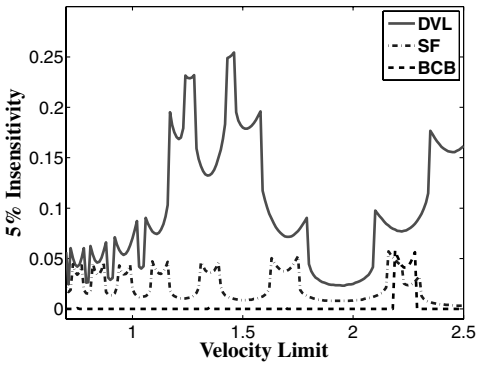

Fig. 17 Insensitivity of 5% vs velocity limit.

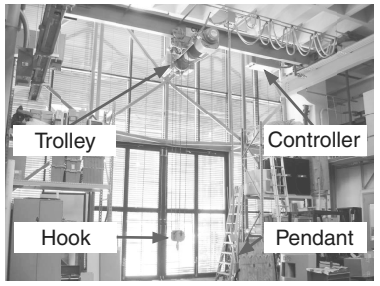

Fig. 18 10-ton bridge crane at Georgia Tech.

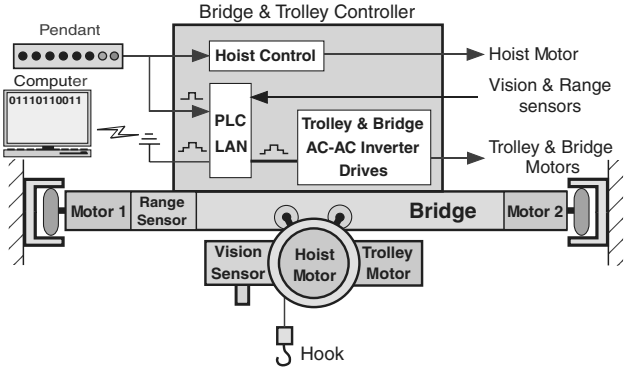

Fig. 19 Hardware configuration.

velocity limit, as expected. The move durations of SF commands abruptly jump after $V_L = 2.25$ to approximately the same speed as the DVL commands due to the increment of the m value in Eq. (16). These data indicate that the move duration of the SF commands is located between the DVL and BCB commands.

Figure 14 demonstrates that the BCB commands induce large residual vibration. As with the case for varying move distance, the BCB commands periodically induce no residual vibration. Both the DVL and SF commands always produce zero residual vibration.

Figure 15 shows that the BCB commands produce less total oscillations as the velocity limit increases toward 2.2 and then it increases after that. On the other hand, the DVL and SF commands linearly increase with velocity limit. The SF commands after $V_L = 2.25$ produce more vibrational energy than the DVL commands.

Figure 16 shows the maximum transient deflection as a function of velocity limit. The DVL commands induce constant deflection and the SF and BCB commands generate much higher deflection over the range shown. As designed, the DVL commands induce constant transient deflection over the ranges of move distance and velocity limit shown in Figs. 10 and 16. After $V_L = 2$, the SF commands induce the same transient deflection as the BCB commands.

Figure 17 shows the 5% insensitivity as a function of velocity limit. The DVL commands have much higher robustness than the SF commands. Note that from about 2.2–2.3, the BCB command cancels vibration (as shown in Fig. 14 and has some measurable robustness in this isolated region.

IV. Experimental Verification

A. Experimental Setup

Experimental evaluation was performed using the 10-ton industrial crane at Georgia Tech shown in Fig. 18. Its workspace is 6.2 m high, 9 m wide, and 42 m long. Figure 19 shows a schematic diagram of the crane equipped with an advanced control system. A Siemens programmable logic controller (PLC) is connected to a laptop computer by a wireless local area network to perform the proposed algorithms. The velocity commands generated by the PLC are then sent to the trolley/bridge motor drives. The drives use the incoming commands from the PLC as velocity set points for the motors. The trolley/bridge control system has Siemens Masterdrives Series AC-AC inverters which use a pulse-width-modulated signal to accurately control the inverter-duty capable motors. To measurement the trolley and payload positions, the control system has a laser range sensor and a Siemens machine vision system.

For these experiments, the suspension cable was approximately 5.0 m in length. The mass of the hook was approximately 50 kg. With this setup, the natural frequency is $\omega = 1.4$ rad/s. Crane operation is based on velocity commands; therefore, the input commands designed with this setup and $D_L = 0.3$ were converted into velocity commands with the maximum velocity set to $V_L = 0.339$ m/s. The maximum acceleration, α, was 0.678 m/s^2 and a sampling time of 35 ms was used. In each experiment, the hook oscillation was measured by the overhead camera.

B. Experimental Results

Figure 20 shows that the DVL and SF commands are vastly better than the BCB command for a 2.5-m move distance of the trolley. The DVL and SF commands induce only small vibration magnitudes both during motion and after arriving at the target location. On the other hand, the BCB command does arrive at the target distance about 1 s faster, but with large residual vibration. Note that the small offsets in the final positions are caused by running the crane with velocity commands, rather than position commands.

Figure 21 illustrates the control robustness by showing the residual oscillation amplitude at the end of each command for a range of move distances and two different suspension cable lengths. In these seven experiments, the three commands designed for the cable length of 5.0 m were tested with cable lengths of both 5.0 and 4.0 m. Changing the suspension length from 5 to 4 m induces a +11.8% error in the frequency used to design the command. The DVL and SF commands show an average increase of only 5 cm of residual vibration magnitude when used with the incorrect suspension length. The BCB commands shows large residual oscillation magnitude, which is similar to the theoretical prediction. The DVL commands show slightly better robustness than the SF commands when the system parameters and move distance are varied.

Figure 22 shows the maximum transient deflection as a function of the move distance. As expected from the theoretical evaluation, the

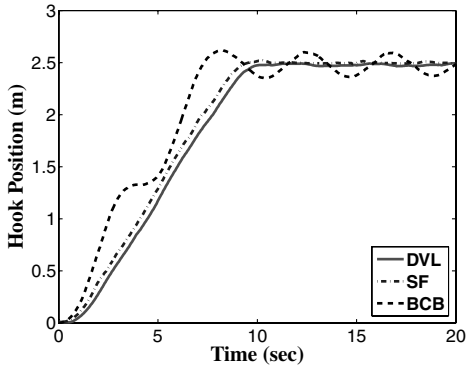

Fig. 20 Experimental time responses of crane hook.

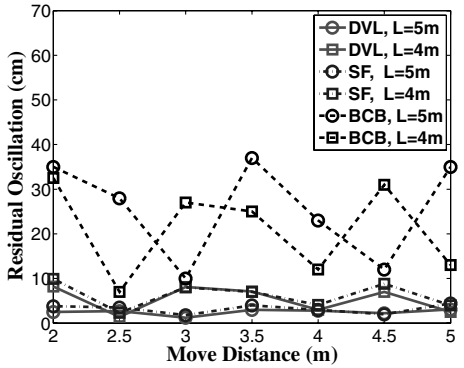

Fig. 21 Experimental residual oscillation of crane hook.

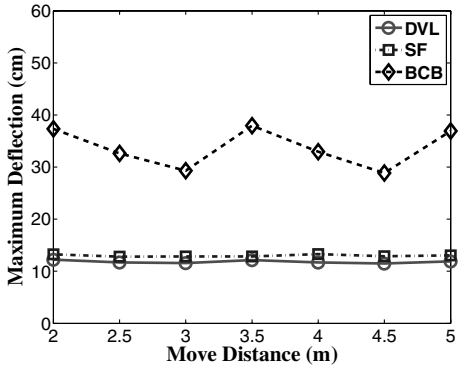

Fig. 22 Experimental maximum deflection of crane hook vs move distance.

DVL commands produce less deflection (an average of 10 cm) than the SF commands (an average of 12 cm) and the BCB commands (an average of 30 cm). The DVL and SF commands produce nearly a constant maximum deflection for the entire operational range, as was predicted by Figs. 10 and 16.

V. Conclusions

An analytical method to generate deflection-limiting commands for systems with velocity limits was developed. By employing the deflection-velocity-limiting shaper, the command profiles greatly reduce residual vibration for rest-to-rest motion of oscillatory systems. When compared to specified-fuel commands, the proposed closed-form commands produce less residual oscillation, less transient deflection, and better robustness to modeling errors. The most significant advantage is that the deflection-velocity-limiting commands are given in closed form. In addition, there is no need to perform a numerical optimization for every possible move distance. The deflection-velocity-limiting commands were validated by both numerical and experimental implementations.

Acknowledgments

This study was supported (in part) by research funds from Chosun University, 2007. The authors would like to thank Siemens Energy and Automation for their support of this work.

References

[1] Singh, G., Kabamba, P. T., and McClamroch, N. H., "Planar, Time-Optimal, Rest-to-Rest Slewing Maneuvers of Flexible Spacecraft," *Journal of Guidance, Control, and Dynamics*, Vol. 12, No. 1, 1989, pp. 71–81.

[2] Liu, Q., and Wie, B., "Robust Time-Optimal Control of Uncertain Flexible Spacecraft," *Journal of Guidance, Control, and Dynamics*, Vol. 15, No. 3, 1992, pp. 597–604.

[3] Ben-Asher, J., Burns, J. A., and Cliff, E. M., "Time-Optimal Slewing of Flexible Spacecraft," *Journal of Guidance, Control, and Dynamics*, Vol. 15, No. 2, 1992, pp. 360–367.

[4] Singh, T., and Vadali, S. R., "Robust Time-Optimal Control: A Frequency Domain Approach," *Journal of Guidance, Control, and Dynamics*, Vol. 17, No. 2, 1994, pp. 346–353.

[5] Tuttle, T., "Creating Time-Optimal Commands for Linear Systems," Ph.D. Thesis, Massachusetts Institute of Technology, Cambridge, MA, 1997.

[6] Tuttle, T., and Seering, W., "Experimental Verification of Vibration Reduction in Flexible Spacecraft Using Input Shaping," *Journal of Guidance, Control, and Dynamics*, Vol. 20, No. 4, 1997, pp. 658–664.

[7] Singhose, W., Banerjee, A., and Seering, W., "Slewing Flexible Spacecraft with Deflection-Limiting Input Shaping," *Journal of Guidance, Control, and Dynamics*, Vol. 20, No. 2, 1997, pp. 291–298.

[8] Wie, B., Sinha, R., Sunkel, J., and Cox, K., "Robust Fuel- and Time-Optimal Control of Uncertain Flexible Space Structures," *Proceedings of the Guidance, Navigation, and Control Conference*, AIAA, Washington, D.C., 1993, pp. 939–948.

[9] Singhose, W., Bohlke, K., and Seering, W., "Fuel-Efficient Pulse Command Profiles for Flexible Spacecraft," *Journal of Guidance, Control, and Dynamics*, Vol. 19, No. 4, 1996, pp. 954–960.

[10] Singh, T., "Fuel/Time Optimal Control of the Benchmark Problem," *Journal of Guidance, Control, and Dynamics*, Vol. 18, No. 6, 1995, pp. 1225–1231.

[11] Pao, L. Y., and Singhose, W., "Verifying Robust Time-Optimal Commands for Multi-Mode Flexible Spacecraft," *Journal of Guidance, Control, and Dynamics*, Vol. 20, No. 4, 1997, pp. 831–833.

[12] Singer, N., Singhose, W., and Kriikku, E., "An Input Shaping Controller Enabling Cranes to Move Without Sway," *American Nuclear Society 7th Topical Meeting on Robotics and Remote Systems*, NTIS, Springfield, VA, 1997.

[13] Singhose, W., Derezinski, S., and Singer, N., "Extra-Insensitive Input Shapers for Controlling Flexible Spacecraft," *Journal of Guidance, Control, and Dynamics*, Vol. 19, No. 2, 1996, pp. 385–391.

[14] Kojima, H., and Singhose, W., "Adaptive Deflection-Limiting Control for Slewing Flexible Space Structures," *Journal of Guidance, Control, and Dynamics*, Vol. 30, No. 1, 2007, pp. 61–67. doi:10.2514/1.23668

[15] Robertson, M., and Singhose, W., "Specified-Deflection Command Shapers for Second-Order Position Input Systems," *Journal of Dynamic Systems, Measurement, and Control*, Vol. 129, Nov. 2007, pp. 856–859. doi:10.1115/1.2789476

[16] Sung, Y-G., and Singhose, W., "Closed-Form Specified-Fuel Commands for Two-Mode Systems," *Journal of Guidance, Control, and Dynamics*, Vol. 30, No. 6, 2007, pp. 1590–1596. doi:10.2514/1.29954

[17] Singhose, W., Biediger, E., Okada, H., and Matunaga, S., "Closed-Form Specified-Fuel Commands for On-Off Thrusters," *Journal of Guidance, Control, and Dynamics*, Vol. 29, No. 3, 2006, pp. 606–611.

[18] Singer, N. C., and Seering, W. P., "Preshaping Command Inputs to Reduce System Vibration," *Journal of Dynamic Systems, Measurement, and Control*, Vol. 112, March 1990, pp. 76–82.

[19] Singhose, W., Singer, N., and Seering, W., "Time-Optimal Negative Input Shapers," *Journal of Dynamic Systems, Measurement, and Control*, Vol. 119, June 1997, pp. 198–205.

[20] Smith, O. J. M., *Feedback Control Systems*. McGraw–Hill, New York, 1958.